




PAPER

Possible quantized charge pump in bilayer and trilayer graphene

Mei-Juan Wang¹, Jun Wang^{1,3}  and Jun-Feng Liu^{2,3}¹ Department of Physics, Southeast University, Nanjing 210096, People's Republic of China² Department of Physics, Guangzhou University, Guangzhou, 510006, People's Republic of China³ Authors to whom any correspondence should be addressed.E-mail: jwang@seu.edu.cn and phjfliu@gzhu.edu.cn**Keywords:** quantized pump, charge transport, multilayer graphene, noninteracting electron systemRECEIVED
28 October 2019REVISED
1 January 2020ACCEPTED FOR PUBLICATION
9 January 2020PUBLISHED
23 January 2020

Original content from this work may be used under the terms of the [Creative Commons Attribution 4.0 licence](https://creativecommons.org/licenses/by/4.0/).

Any further distribution of this work must maintain attribution to the author(s) and the title of the work, journal citation and DOI.

**Abstract**

We report a theoretic study of the two-parameter adiabatic charge pump based on the bilayer and trilayer graphene systems. The two perpendicular time-dependent electric fields with a phase lag between them are taken as the pumping potentials, which induce an instant energy gap in each pumping region. Based on both a continuum model and a lattice model, we show that the pumping results from the bilayer and trilayer graphene systems are very different when the Fermi energy happens to reside in the opened energy gap: there is no pumping current for the bilayer system whereas a quantized charge pumping effect emerges in the trilayer-graphene based pump device. This difference can be accounted for by the different Berry phases of Dirac electrons in the two systems. Our findings may shed a light on developing a quantized charge pumping device.

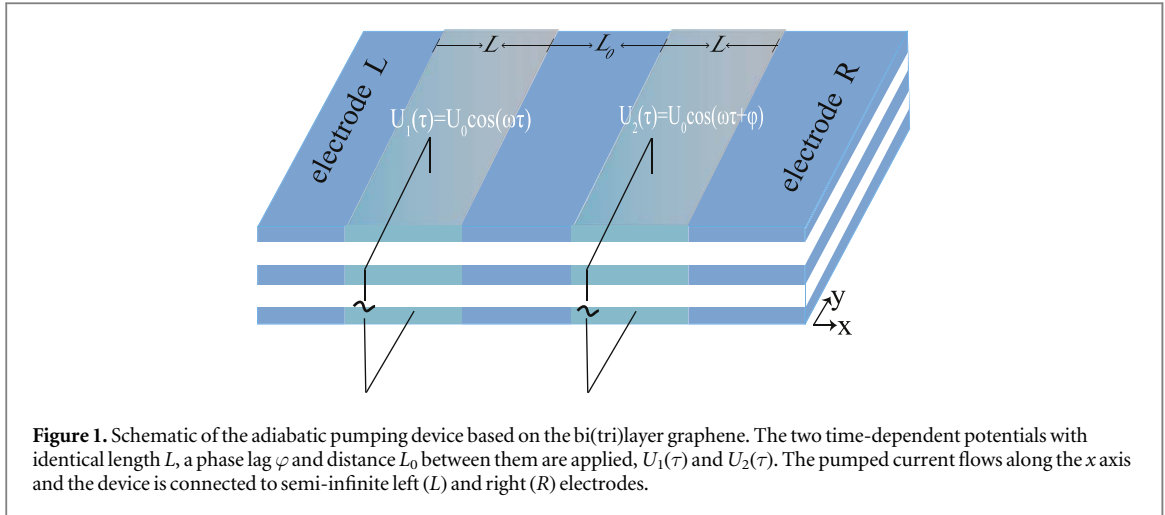
1. Introduction

Since a single layer of graphite isolated successfully in 2004 [1], graphene has attracted swiftly a great interest in condensed matter physics. As both the thinnest and the strongest material ever measured [2], graphene further ignited the research of the devices based on carbon material [3, 4]. Moreover, the particles have a linear energy dispersion around the band center that can be described by a massless Dirac equation leading to many peculiar transport properties [5]. The Carbon atoms are assembled into a hexagonal lattice with a unit cell comprising the two site-inequivalent Carbon atoms [6], which can be regarded as pseudospin, another degree of freedom in addition to the valley and spin. In the last several years, the bilayer (BLG) and trilayer graphene (TLG) have attracted much attention of researchers [7, 8]. A striking feature is the stacking arrangement of graphene layers which fundamentally changes the electronic properties of multilayer graphene [9–11]. And it has been demonstrated systematically that the band gap of the multilayer graphene with rhombohedral stacking can be controlled by a perpendicular electric field [12–15].

The transport properties of multilayer graphene have also been extensively and intensively studied in literatures [16–18], and much different and unconventional transport phenomena were predicted. Among those is the quantum pumping effect of the electric charge, spin and valley degree of freedom on the multilayer graphene system [19–25]. E.g. Chan [26] and coauthors studied the possible layer polarization pump in a BLG system, and they regarded the graphene layer as one pseudospin degree of freedom in order to obtain the pseudospin polarized pumping currents by a perpendicular time-dependent electric field.

In the field of the quantum parameter pump, researchers are paying much attention to the quantized pump effect, i.e. an integer number of charges are pumped out in a pumping cycle because the pumping quantization is quite desirable in building a standard of electric current. For the noninteracting electron system, the Thouless topological pump [27] is the first proposal stating that a one-dimensional (1D) moving potential can pump out an integral charge when the Fermi energy lies in the energy gap opened by the moving potential. Recently, several research groups [28–31] have independently observed such quantized pump in 1D optical superlattice or cold-atom systems. However, it is still a challenge to implement such an experiment in the electron system, because it is quite difficult to control the varying potential precisely in experiments.

In a previous work [32], two of the authors investigated a new pumping scheme for the quantized charge pump in the monolayer graphene system, and they concluded that the pump is quantized as long as the pumping



potential can induce an energy gap of the Dirac electrons. However, it is practically difficult in experiment to generate a time-dependent staggered potential in the monolayer graphene. On the contrary, one can easily employ a perpendicular electric field to induce a staggered potential in a multilayer graphene system [12–15], and the potential difference among layers will open an energy gap of the electrons. Therefore, it is desirable to study whether the quantized pump found in the monolayer graphene [32] is automatically applicable to the multilayer graphene device.

In this work, we study the charge pumping effect in some typical multilayer graphene systems like the BLG and TLG, which are chosen as the base materials for the pumping device as examples. By using the Büttiker–Prère–Thomas (BPT) pumping formula [33] in the adiabatic limit, we calculate the pumping current in both a continuum model and a lattice model and show that the pumping results from the BLG and TLG systems are almost opposite. The quantized pump is only found in the TLG system whereas there is no any pumping current in BLG system when the Fermi energy resides in the energy gap opened by the applied pumping potentials. The drastically contrary results stem from the different Berry phases of the massive Dirac electrons in the BLG and TLG.

The paper is organized as follows. In section 2 we introduce a simplified model for bi(tri)layer graphene and work out the consequences on the pumping current. In section 3 we discuss the results for the continuum model on account of the two-band Hamiltonian of multilayer graphene. The discussions and conclusions are presented in section 4.

2. Lattice model

In order to systematically examine the pumping effect in the multilayer graphene system, we consider a traditional two-parameter pumping device based upon Bernal(AB)-stacked BLG and rhombohedral(ABC)-stacked TLG. The pumping setup is composed of two electrodes and two pumping regions, which are separated within a length of L_0 and subjected to the time-dependent pumping potentials $U_{i=1,2}$ on the outermost regions as shown in figure 1, which can be implemented by perpendicular electric fields via capacitors. As a result, the staggered potential in each layer due to the electric field will open an energy gap of Dirac electrons in the local pumping regions. This energy gap is the prerequisite for possible pumping quantization in the monolayer graphene system [32].

We first consider a lattice model to calculate the possible pumping current flowing through the BLG and TLG device in figure 1. Actually, the features of the low-energy Dirac electrons depend crucially on the stacking style of multilayer graphene. In this work, the AB(C) stacking is chosen because the energy gap can be opened much easier due to the applied electric field [11]. And we just take the nearest hopping terms in interlayer and intralayer into account, since the trigonal warping effects has little effect on our study. The low-energy bands can be described by an effective tight-binding Hamiltonian [34]

$$H = -t \sum_{\langle ij \rangle, n} C_{i,n}^\dagger C_{j,n} + \gamma_1 \sum_{ij, n \neq n'} C_{i,n}^\dagger C_{j,n'} + \sum_{i,n} U_\tau(i) \mu_n C_{i,n}^\dagger C_{i,n}. \quad (1)$$

Here, the first and second terms describe pristine multilayer graphene, $\langle ij \rangle$ stands for the nearest-neighboring sites, $C_{i,n}^\dagger$ ($C_{i,n}$) is the creation (annihilation) operator at site i in the n th layer, $n(n' = n \pm 1)$ is the layer index, t is the nearest hopping energy in the same layer, and $\gamma_1 = 0.13t$ is the vertical hopping energy between the nearest layers. The third term is the time-dependent pumping potentials induced by the perpendicular electric field,

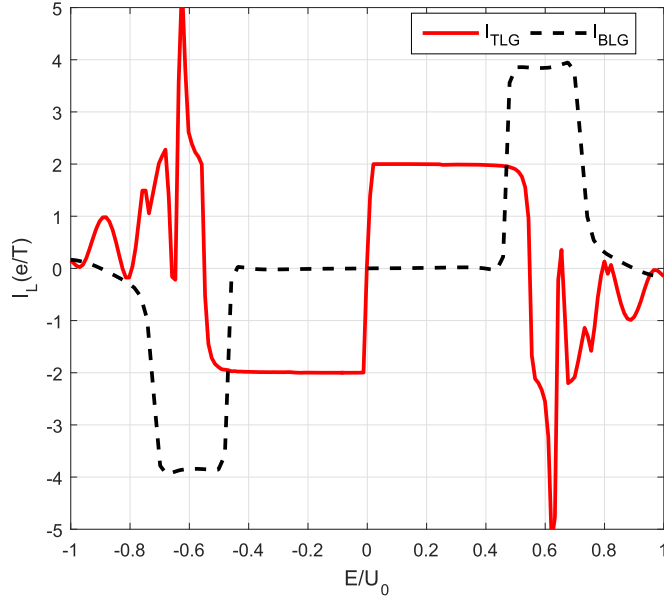


Figure 2. Color plot of the pumping current I_L as a function of E in BLG device (black-dashed line) and TLG device (red-solid line). The width of device is $N_y = 48$. Other parameters are $U_0 = 0.1\gamma_1$, $\varphi = \pi/2$, $L = 150a$, and $L_0 = 0$ with a being the lattice constant.

$\mu_n = +(-)1$ for the bottom (top) layer for simplicity, i.e. the top and bottom layers of the BLG and TLG have opposite on-site potential energy while a zero energy potential is assumed in the middle layer of the TLG

$$U_\tau(i) = \begin{cases} U_0 \cos(\omega\tau), & i \in (0, L) \\ U_0 \cos(\omega\tau + \varphi), & i \in (L + L_0, 2L + L_0) \\ 0, & \text{others,} \end{cases}$$

where U_τ is homogeneous in the finite-length L region, U_0 is the pumping strength, and φ is the pumping phase shift. L_0 is assumed to be the region length between two pumping areas. The frequency of the potential modulation ω assumed to be infinitesimal since the adiabatic pump is considered in this work. Similar to the monolayer graphene [32], the pumping potentials with opposite signs will generate a topological interface state between the two pumping regions, which are critical to generate a quantized charge current when the Fermi energy lies in the energy effect gap opened by the pumping potentials U_τ . The BPT formula [33] is employed here to calculate the pumping current in adiabaticity

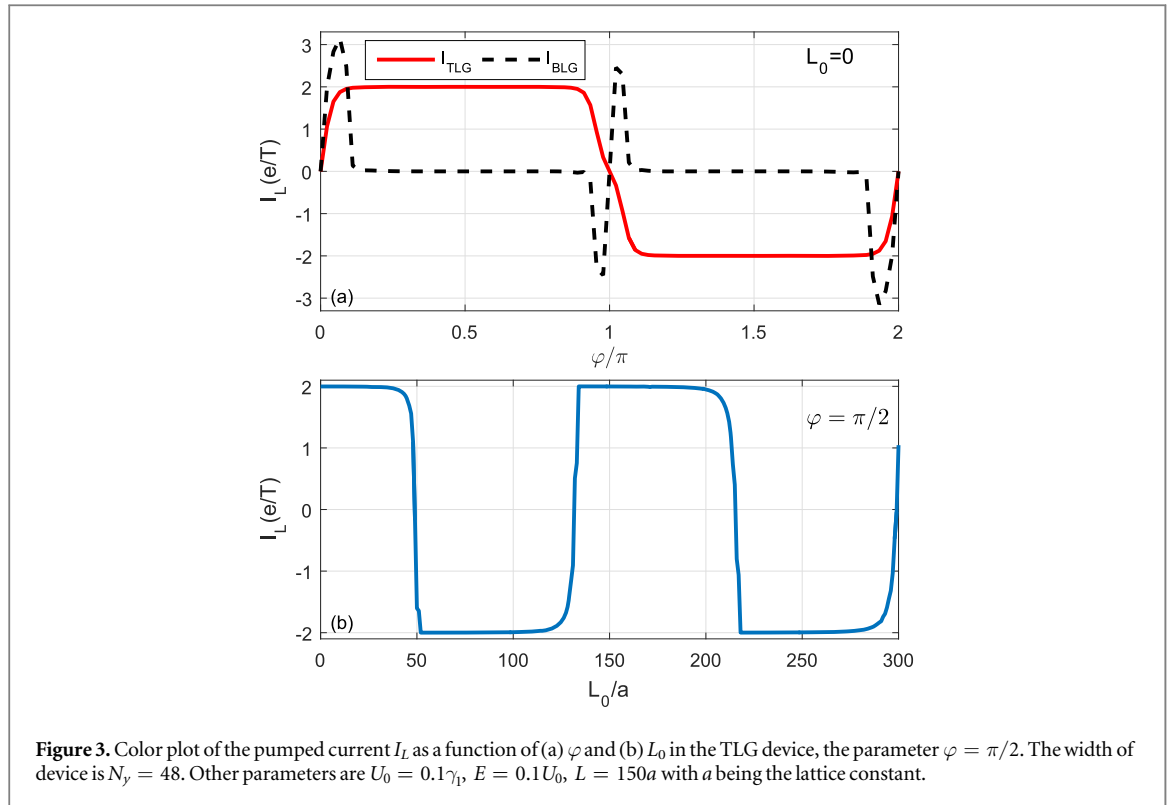
$$I_\alpha = \frac{ie}{2\pi T} \int_0^T d\tau \text{Tr} \left(\frac{\partial \mathcal{S}_\tau}{\partial \tau} \mathcal{S}_\tau^* \right)_{\alpha, \alpha}, \quad (2)$$

where \mathcal{S}_τ is the instantaneous scattering matrix with α being the left or right electrode index, $\alpha = L, R$, and $T = 2\pi/\omega$ is the pumping cycle. In order to carry out numerical calculations by the convenient Green's function method, the above equation can be written as [32]

$$I_\alpha = \frac{e}{2\pi T} \oint_0^T d\tau \text{Tr} (\Gamma G_\tau^r \dot{U}_\tau G_\tau^a)_{\alpha, \alpha}, \quad (3)$$

where $\Gamma_\alpha = i(\Sigma_\alpha - \Sigma_\alpha^+)$ is the line-width matrix of the semi-infinite electrode α , and Σ_α is its corresponding self-energy function. $G_\tau^{r(a)} = [E \pm i0^\pm - \mathcal{H}_\tau]^{-1}$ is the instantaneous retarded (advanced) Green's function of the two-terminal device, $\dot{U}_\tau = dU_\tau/d\tau$ is the time derivative of pumping potentials, and the trace is over the transverse sites of a unit slice of the lattice pumping model. The Green's function $G_\tau^{r(a)}$ can be calculated by using usual recursive Green's function method [35] since the model device can be decomposed into three parts of left and right electrodes as well as the scattering region.

We perform our calculations in a finite-width N_y device and present the pumping current I_L in both the BLG and TLG devices versus the Fermi energy E in figure 2. In numerics, the pumping strengths are set as the same $U_0 = 0.1\gamma_1$, the interlayer hopping energy set as $\gamma_1 = 0.13t$, while the in-plane hopping energy is set as $t = 1$ eV as the energy unit, and the ambient temperature is taken as zero. In figure 2, the red-solid line represents the pumping result in the TLG system and the current is quantized when the Fermi energy is around the Dirac point ($E = 0$). This is the same as the $I_L - E$ curve of the monolayer-graphene pumping device [32] that the platform value is $\pm 2e/T$, which indicates that in a pumping cycle, two charges are pumped out. Here, the 'two' denotes the valley degeneracy in the graphene system. In contrast, one can see that there is no current flowing around the band center $E \sim 0$ from the black-dashed line representing the BLG case. This is drastically contrary to the



pumping result of the TLG device. When $E \gtrsim |0.4U_0|$ that the Fermi energy locates outside of the effective gap, the pumping current for the BLG begins to raise up but the pumping value is not quantized, and this is just a usual quantum parameter pump. It is noted here that in our calculations, only one transverse mode is involved in the transport because the Fermi energy is near to the charge neutral point and a narrow lattice ribbon with $N_y = 48$ is considered, where N_y is the atom number in a transverse one-layer atom chain.

It is seen that the zero-current platform in the BLG system and the quantized platform in the TLG one almost occur in the same energy region around the original Dirac point. It is clear that the quantized platform stems from the Fermi energy locating the effective energy gap opened by the pumping potential U_τ , which are the same as the monolayer graphene case [32]. Certainly, the energy maximum value for the quantized platform is much less than the theoretic value $U_0/\sqrt{2}$ and this is related to fact that the effective gap in the multilayer graphene would decrease with the increasing layer number [14]. Outside the effective energy gap, the pumping results are not quantized and meanwhile, the instant transmission would not keep zero in a pumping cycle. The zero pumping current $I_L = 0$ in the bilayer system is very different from the odd-number layer of the graphite system like the monolayer and TLG systems. This is related to the Berry phase of electrons responsible for the pumping current and we will return to it in next subsection.

In comparison with the monolayer graphene pumping, we also study the pumping current I_L as a function of phase difference φ . The essential parameter φ guarantees the gap opened in the whole pumping period, which is the prerequisite of the pumping quantization. In figure 3(a), the pumping current is present for the TLG case and it is seen that except for $\varphi \sim n\pi$ (n , integer), I_L is quantized. Oppositely, there is still no current pumped out from the BLG device as illustrated, and only for $\varphi \sim n\pi$ is a nonzero pumped current seen, where the effective energy gap is so small and the Fermi energy may locate outside of it in some time interval of the pumping cycle.

The results obtained above is under the condition that the distance $L_0 = 0$ between the two pumping regions. It may be difficult to apply the electric field on the two regions abruptly. Therefore, we consider the current versus a finite separation L_0 in the TLG device. From figure 3(b), one can see the current exhibits an alternative effect from $-2e/T$ to $+2e/T$ with the variation of L_0 . It indicates that the distance length only affects the signs of the current but not the quantized feature, which may provide a practical convenience for the experimental measurement. Certainly, we can even employ a gate voltage to modulate the local potential in the middle region between two pumping potentials, which can in turn controls and reverses the pumping results. The reason is the dynamic phase of electrons traveling the graphene will contribute to the pumping phase difference φ .

3. Continuum model

In order to get some insight on the reason that there is no pumping current in the BLG system, we here utilize a two-band approximate Hamiltonian [36] of the multilayer graphene to further analyze the pumping effect. This is feasible because the low-energy behavior of electrons near the Dirac point is our concern. The continuum Hamiltonian reads

$$H = \begin{pmatrix} U_\tau & \frac{(\hbar v_f)^{N_z}}{(-\gamma_1)^{(N_z-1)}}(k_x - i\eta k_y)^{N_z} \\ \frac{(\hbar v_f)^{N_z}}{(-\gamma_1)^{(N_z-1)}}(k_x + i\eta k_y)^{N_z} & -U_\tau \end{pmatrix}, \quad (4)$$

here, $N_z = 2(3)$ is the layer number, $\eta = \pm 1$ is the valley index. It is noted that we take only one valley into account ($\eta = 1$) because of the valley degeneracy. k_x, k_y are the in-plane momentum. $(k_x^2 + k_y^2)^{N_z} = (E^2 - U_\tau^2) \times \left[\frac{(-\gamma_1)^{N_z-1}}{(\hbar v_f)^{N_z}} \right]^2$, so there are $2N_z$ different values for k_x . Since we consider the adiabatic limit, the transverse momentum k_y is assumed to conserve in the instantaneous scattering process. In the above lattice model with a finite width, there is only one propagating mode active. Therefore, we just focus on the normal incidence $k_y = 0$ in the following. In fact, the larger k_y the electrons have, the more liable the pumping quantization is, because in the effective gap the evanescent wavevector (momentum) becomes larger with an increase of k_y , and the transmission easily damps to zero.

We take the calculation of reflection in the TLG ($N_z = 3$) as example. From the Hamiltonian we can also get the wavefunction

$$\Psi = \sum_{j=1}^3 a_{j\pm} \left(\frac{(\pm k_j)^3}{(E - U_\tau)(-\gamma_1)^2 / (\hbar v_f)^3} \right) e^{\pm i k_j x} \quad (5)$$

$$= P\varepsilon(x)C, \quad (6)$$

with matrices

$$P = \begin{bmatrix} \frac{(k_1)^3(\hbar v_f)^3}{(E - U_\tau)(-\gamma_1)^2} & \frac{(-k_1)^3(\hbar v_f)^3}{(E - U_\tau)(-\gamma_1)^2} & \frac{(k_2)^3(\hbar v_f)^3}{(E - U_\tau)(-\gamma_1)^2} & \frac{(-k_2)^3(\hbar v_f)^3}{(E - U_\tau)(-\gamma_1)^2} & \frac{(k_3)^3(\hbar v_f)^3}{(E - U_\tau)(-\gamma_1)^2} & \frac{(-k_3)^3(\hbar v_f)^3}{(E - U_\tau)(-\gamma_1)^2} \\ 1 & 1 & 1 & 1 & 1 & 1 \end{bmatrix}, \quad (7)$$

$$\varepsilon(x) = \text{Diag}[e^{ik_1x}, e^{-ik_1x}, e^{ik_2x}, e^{-ik_2x}, e^{ik_3x}, e^{-ik_3x}], \quad (8)$$

and

$$C = [a_{1+}, a_{1-}, a_{2+}, a_{2-}, a_{3+}, a_{3-}]^T, \quad (9)$$

here, $+/-$ indicates the right/left propagating or evanescent states, the momentum $k_1 = [(E^2 - U_\tau^2)\gamma_1^4]^{1/6}/(\hbar v_f)$, $k_2 = (-1/2 + \sqrt{3}i/2)k_1$, $k_3 = (1/2 + \sqrt{3}i/2)k_1$. We acquire the reflection and transmission coefficient by utilizing the boundary conditions [16]

$$\begin{cases} \Psi_I = \Psi_{II}, \frac{\partial \Psi_I}{\partial x} = \frac{\partial \Psi_{II}}{\partial x}, \frac{\partial^2 \Psi_I}{\partial x^2} = \frac{\partial^2 \Psi_{II}}{\partial x^2}, & x = 0, \\ \Psi_{II} = \Psi_{III}, \frac{\partial \Psi_{II}}{\partial x} = \frac{\partial \Psi_{III}}{\partial x}, \frac{\partial^2 \Psi_{II}}{\partial x^2} = \frac{\partial^2 \Psi_{III}}{\partial x^2}, & x = L, \\ \Psi_{III} = \Psi_{IV}, \frac{\partial \Psi_{III}}{\partial x} = \frac{\partial \Psi_{IV}}{\partial x}, \frac{\partial^2 \Psi_{III}}{\partial x^2} = \frac{\partial^2 \Psi_{IV}}{\partial x^2}, & x = L + L_0, \\ \Psi_{IV} = \Psi_V, \frac{\partial \Psi_{IV}}{\partial x} = \frac{\partial \Psi_V}{\partial x}, \frac{\partial^2 \Psi_{IV}}{\partial x^2} = \frac{\partial^2 \Psi_V}{\partial x^2}, & x = 2L + L_0, \end{cases}$$

where Ψ_{I-V} are the wavefunctions in the left electrode, the left potential island, the normal L_0 region, the right potential island, and the right electrode, respectively. For the electrode L and electrode R of the TLG device, the vectors C_L and C_R can be expressed as $C_L = [1 \ r_1 \ 0 \ r_2 \ 0 \ r_3]^T$, $C_R = [t_1 \ 0 \ t_2 \ 0 \ t_3 \ 0]^T$.

Through numerical calculations, we discover that the incident electron is fully reflected with $|r_1| = 1$ when the Fermi energy is in the gap, as a result, we utilize $r = r_1$ in the following consideration and neglect the contribution from the transmission. Finally, the formula of the pumping current in equation (2) can be rewritten as

$$I_L = \frac{ie}{2\pi T} \oint_T d\tau \left(\frac{\partial r}{\partial \tau} r^* \right). \quad (10)$$

As is known, the pumping current equals the area enclosed by the directional trajectories of r on the complex plane from the current formula expression. The trajectory goes around clockwise or anticlockwise meaning positive or negative pumping current.

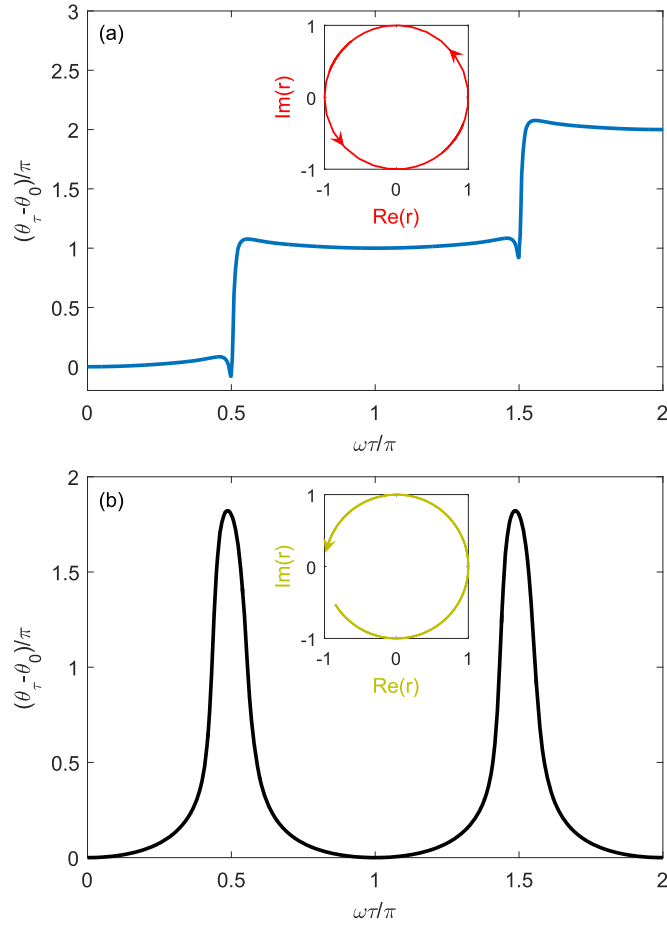
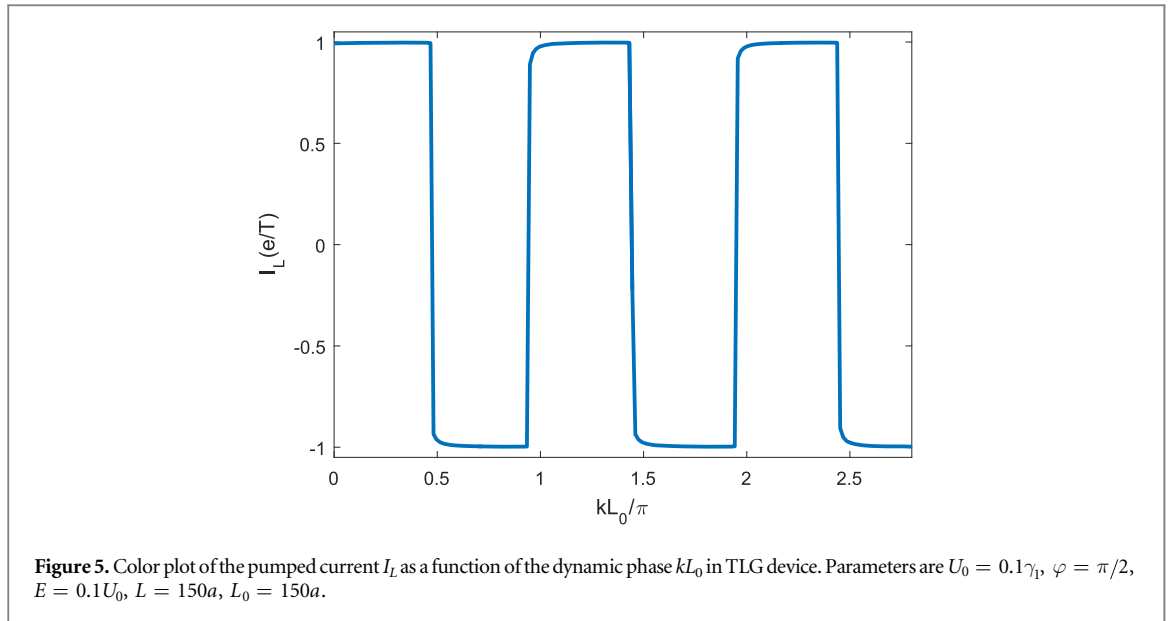


Figure 4. Color plot of argument of the complex reflection amplitude ($\theta_\tau = \arg(r)$) as a function of time $\omega\tau$ in one period for (a) TLG device and (b) BLG device. The insets present the trajectory of r on complex plane in a cycle. Parameters are $U_0 = 0.1\gamma_1$, $\varphi = \pi/2$, $E = 0.1U_0$, $L_0 = 150a$.

In figure 4, we plot the argument $\theta_\tau = \arg(\Re(r) + i\Im(r))$ of r as a function of $\omega\tau$ and its trajectory [25, 37]. It is seen that the magnitude of the reflection always equals 1 for the TLG and BLG systems. For the TLG device, θ_τ increases to 2π in a pumping cycle and the track of r is a unit circle on the complex plane as shown in figure 4(a). Reversely, a different situation appears in figure 4(b) where the BLG device is studied, θ_τ goes back to the initial value after going through a cycle. The track of r does not enclose a finite area. This clearly indicates that the winding number of the reflection coefficient r is equal to 1 for the TLG device but 0 for the BLG one. Therefore, the pumping results are equal to be 1 or 0 in the two cases.

To further show the quantized pump, we present the pumping current I_L as a function of the dynamic phase kL_0 of electrons traveling in the pristine graphene region between the two time-dependent potentials, $k = [(E + V_0)^2 \gamma_1^4]^{1/6} / (\hbar v_f)$, where V_0 is a gate voltage to modulate the local momentum. In figure 5, I_L exhibits the same quantized magnitude e/T and the current direction can be reversed with the dynamic phase kL_0 , which is consistent with results shown in figure 3(b). The results validate the quantized pumping effect found in the TLG lattice model.

When the argument θ_τ of r advances 2π , the system can pump out a charge while it advances zero in a pumping cycle, the pumped charge is zero. From this perspective, the former case of the TLG with an applied staggered potential is a topologically nontrivial while the BLG is a trivial system. As a matter of fact, the Berry phase of the TLG electrons is 3π while it is 2π for the BLG electrons [38]. Together with the quantized pump found in the monolayer graphene [32], where the Berry phase of electrons is also π , we can conclude that the even-number-layer multilayer graphene with Berry phase $\gamma = n\pi$ (n , even number) cannot lead to the reflection coefficient exhibiting a phase reversal, or the 2π phase increment in a pumping cycle responsible for the quantized pump. However, the odd-number-layer system can pump out an integer number of charge. Because the incident wavefunction of electrons has a π phase difference from the reflected wavefunctions in the scattering event upon with the pumping potentials, which means the quantum states in the pumping region experience a 2π increment and keep in the same state with a charge pumped out of the system.



It has been argued in the literatures [32, 39] that the topological interface state between the two pumping potentials is upmost important for the possible quantized pumping effect. However, one can see that the electron properties in the device also play a vital role for the formation of the quantized pump. If the Berry phase of electrons is not equal to π , the pumping current may even not occur since the phase of the reflection coefficient does not advance 2π in a pumping cycle. Alternatively, the electrons with an ordinary Berry phase $n\pi$ (n , even number) does not produce any exotic results. As a matter of fact, there still exists an interface state bridging two opposite staggered-potential regions in the BLG system, which has been observed in experiment recently [40]. Hence, it is concluded that the topological interface state is not a unique prerequisite for the pumping quantization for such a two-parameter pumping device. Note for the aforementioned two models in [32, 39], the monolayer graphene and the nanowire superlattice with Rashba spin orbit interaction, the electrons happen to possess a π Berry phase so that the quantized pumping effect is feasible.

Due to the layer structure, the energy band can be easily opened in the both the trilayer and BLG by using a perpendicular electric field in comparison with the monolayer graphene. A tunable energy gap of the TLG was reported by several experimental works [13, 41] and the observed gap can be as large as about 120 meV. Such a large gap is quite favorable for the pump quantization proposed in this work since the Fermi energy can easily keep in the gap in the whole pumping cycle, and moreover, the temperature effect cannot smear the gap readily, either.

4. Conclusion

In conclusion, we have comparatively studied the charge pumping effect in both the TLG and BLG materials. The pumping results are strikingly different for these two systems. For the BLG device, there is no pumping current at all when the Fermi energy locates in the effective energy gap opened by the pumping potentials, but it is exactly quantized within the same parameters for the TLG case. It is believed that the different Berry phases of the Dirac electrons in these two systems account for such distinct pumping results. Our findings might shed a new insight on the quantized pumping effect.

Acknowledgments

This work is supported financially by the NSFC with Grant Nos. 11574045, 11774144, and 11874221.

ORCID iDs

Jun Wang  <https://orcid.org/0000-0002-6278-0677>

References

- [1] Novoselov K S, Geim A K, Morozov S V, Jiang D, Zhang Y, Dubonos S V, Grigorieva I V and Firsov A A 2004 *Science* **306** 666–9
- [2] Geim A K 2009 *Science* **324** 1530–4

- [3] Geim A and Novoselov K 2007 *Nat. Mater.* **6** 183–91
- [4] Chen D, Tang L and Li J 2010 *Chem. Soc. Rev.* **39** 3157–80
- [5] Shen S Q 2018 *Topological Insulators: Dirac Equation in Condensed Matter* (Berlin: Springer)
- [6] Cooper D R et al 2012 *ISRN Condens. Matter Phys.* **56** 501686
- [7] Nilsson J, Neto A C, Guinea F and Peres N 2008 *Phys. Rev. B* **78** 045405
- [8] Zhang F, Sahu B, Min H and MacDonald A H 2010 *Phys. Rev. B* **82** 035409
- [9] Guinea F, Neto A C and Peres N 2006 *Phys. Rev. B* **73** 245426
- [10] Min H and MacDonald A H 2008 *Phys. Rev. B* **77** 155416
- [11] Bao W et al 2011 *Nat. Phys.* **7** 948
- [12] Mucha-Kruczyński M, McCann E and Fal’ko V I 2010 *Semicond. Sci. Technol.* **25** 033001
- [13] Lui C H, Li Z, Mak K F, Cappelluti E and Heinz T F 2011 *Nat. Phys.* **7** 944
- [14] Tang K, Qin R, Zhou J, Qu H, Zheng J, Fei R, Li H, Zheng Q, Gao Z and Lu J 2011 *J. Phys. Chem. C* **115** 9458–64
- [15] Jung J and MacDonald A H 2013 *Phys. Rev. B* **88** 075408
- [16] Van Duppen B and Peeters F 2013 *Europhys. Lett.* **102** 27001
- [17] Dell’Anna L, Majari P and Setare M 2018 *J. Phys.: Condens. Matter* **30** 415301
- [18] Wang K, Harzheim A, Taniguchi T, Watanabei K, Lee J U and Kim P 2019 *Phys. Rev. Lett.* **122** 146801
- [19] Niu Q and Thouless D 1984 *J. Phys. A: Math. Gen.* **17** 2453
- [20] Low T, Jiang Y, Katsnelson M and Guinea F 2012 *Nano Lett.* **12** 850–4
- [21] San-Jose P, Prada E, Schomerus H and Kohler S 2012 *Appl. Phys. Lett.* **101** 153506
- [22] Jiang Y, Low T, Chang K, Katsnelson M I and Guinea F 2013 *Phys. Rev. Lett.* **110** 046601
- [23] Ingaramo L H and Foa Torres L E 2013 *Appl. Phys. Lett.* **103** 123508
- [24] Napitu B and Thijssen J 2015 *J. Phys.: Condens. Matter* **27** 275301
- [25] Wang M J, Wang J and Liu J F 2019 *Sci. Rep.* **9** 3378
- [26] Wang J, Lu H, Hu Y, Zhao W S, Wang G and Chan K 2017 *J. Phys. D: Appl. Phys.* **50** 205101
- [27] Thouless D 1983 *Phys. Rev. B* **27** 6083
- [28] Lohse M, Schweizer C, Zilberberg O, Aidelsburger M and Bloch I 2015 *Nat. Phys.* **12** 350–4
- [29] Nakajima S, Tomita T, Taie S, Ichinose T, Ozawa H, Wang L, Troyer M and Takahashi Y 2016 *Nat. Phys.* **12** 296–300
- [30] Citro R 2016 *Nat. Phys.* **12** 288
- [31] Ma W, Zhou L, Zhang Q, Li M, Cheng C, Geng J, Rong X, Shi F, Gong J and Du J 2018 *Phys. Rev. Lett.* **120** 120501
- [32] Wang J and Liu J F 2017 *Phys. Rev. B* **95** 205433
- [33] Büttiker M, Thomas H and Prêtre A 1994 *Z. Phys. B* **94** 133–7
- [34] Xu L, Zhou Y and Gong C D 2013 *J. Phys.: Condens. Matter* **25** 335503
- [35] Lewenkopf C H and Mucciolo E R 2013 *J. Comput. Electron.* **12** 203–31
- [36] Barbier M, Vasilopoulos P, Peeters F and Pereira J M Jr 2009 *Phys. Rev. B* **79** 155402
- [37] Zhou C, Zhang Y, Sheng L, Shen R, Sheng D and Xing D 2014 *Phys. Rev. B* **90** 085133
- [38] Koshino M and McCann E 2009 *Phys. Rev. B* **80** 165409
- [39] Wang J, Liu J and Ting C 2019 *Phys. Rev. B* **100** 075402
- [40] Li J, Wang K, McFaul K J, Zern Z, Ren Y, Watanabe K, Taniguchi T, Qiao Z and Zhu J 2016 *Nat. Nanotechnol.* **11** 1060
- [41] Khodkov T, Khrapach I, Craciun M F and Russo S 2015 *Nano Lett.* **15** 4429–33